scientific reports

Check for updates

OPEN

Biomechanical effects of insole material stiffness on the human foot: a finite element analysis

Renbiao Lin[1], Xu Tao[2], Guanghui Wang[2], Jianquan Liu[2], Zhe Zhao[2], Wei Liu[2]✉ & Wencui Li[2]✉

Functional insoles are widely used to redistribute plantar pressure and support the medial arch; however, the biomechanical effects of insole material stiffness remain unclear. This study employed finite element analysis (FEA) to investigate the relationship between insole stiffness and foot tissue loading, providing a theoretical basis for personalized insole design and clinical application. A three-dimensional finite element model of a healthy 26-year-old male foot and insole was reconstructed from CT images. Exploring the trend of the insole material stiffness on foot biomechanics through parametric analysis. Six insole materials with elastic moduli of 100, 260, 1,000, 3,000, 5,000, and 500,000 MPa—were analyzed, The Poisson's ratio for all insole materials was assumed to be 0.45. Two loading conditions, static bilateral stance and gait forefoot contact, were simulated to evaluate foot displacement, plantar stress, and stresses on the medial process of the calcaneal tuberosity and metatarsals. The finite element model demonstrated good agreement with experimental plantar pressure measurements, the experimentally measured peak plantar pressure was 0.2217 MPa, while the finite element model calculated a value of 0.234 MPa, with a relative error of approximately 2%. Both high-stress regions were located at the central area of the heel, and the stress distribution trends were consistent, indicating that the model validation is effective. Increasing insole stiffness reduced foot displacement (48.0%), plantar peak stress (47.5%), calcaneal peak stress (30.8%), and metatarsal peak stress (20.8%). When the elastic modulus exceeded approximately 3,000 MPa, further biomechanical benefits plateaued, indicating a diminishing marginal effect. This study quantitatively characterizes the intrinsic relationship between insole stiffness and foot biomechanics under static and dynamic conditions. The findings provide robust biomechanical evidence to guide personalized insole design, prevent soft tissue overload, and support the clinical application of functional insoles.

Keywords Insole materials, Finite element analysis, Foot biomechanics, Personalized insole design

Abbreviations

FEA	Finite element analysis
SED	Strain energy density

The foot, as a crucial component of the human musculoskeletal system, plays an essential role in weight-bearing, shock absorption, balance maintenance, and propulsion during daily activities and locomotion. Due to prolonged exposure to repetitive mechanical loading, the foot is highly susceptible to soft tissue injuries and chronic overuse disorders, among which plantar heel pain is a common and clinically significant condition[1]. Plantar fasciitis represents the predominant etiology, typically manifesting as stabbing or throbbing pain in the medial heel region, which exacerbates after morning rise, prolonged standing, or extended walking, thereby severely impairing walking ability and quality of life. Epidemiological data indicate that approximately 10% of adults experience plantar fasciitis during their lifetime[2], and its prevalence is particularly high among long-distance runners[3].

Non-surgical interventions are commonly employed to alleviate pain and redistribute plantar stress[4]. Among them, insoles are widely utilized due to their convenience, cost-effectiveness, and favorable biomechanical modulation. Appropriately designed insoles can provide effective arch support, optimize plantar pressure distribution, and significantly enhance wearing comfort and gait stability[5]. However, commercial insoles are highly diverse, and their design largely relies on empirical approaches or trial-and-error methods, particularly regarding the selection of the insole material's Young's modulus, which lacks robust quantitative guidance.

[1]Dehua County Hospital, Quanzhou, Fujian, China. [2]Shenzhen Second People's Hospital, Shenzhen, Guangdong, China. ✉email: footankleliuwei@163.com; 13923750767@163.com

Previous studies have mainly focused on the evaluation of shock absorption and arch support[6], whereas systematic quantitative investigations into how the Young's modulus of insole materials affects foot biomechanical responses remain limited[7], constraining the precision of insole design and its clinical efficacy.

In recent years, finite element analysis (FEA) has emerged as a powerful and accurate approach in biomedical engineering and has achieved remarkable progress in foot biomechanics research[8–10]. Three-dimensional finite element models enable precise simulation of tissue displacement, stress distribution, and overall mechanical responses under controlled material and loading conditions, thereby providing a solid theoretical basis for the optimization of functional insole design and clinical decision-making.

Against this background, the present study aims to systematically investigate the influence of insole material Young's modulus on key foot biomechanical indicators, including foot displacement, plantar stress, medial process of the calcaneal tuberosity stress, and metatarsal stress. A high-fidelity three-dimensional finite element model of a healthy adult male foot was reconstructed from lower limb CT data. Six representative insole materials, covering a wide stiffness spectrum from flexible to highly rigid—Six insole materials with elastic moduli of 100, 260, 1,000, 3,000, 5,000, and 500,000 MPa—were analyzed, The Poisson's ratio for all insole materials was assumed to be 0.45. Two typical loading conditions, static bilateral stance and gait forefoot contact, were simulated to quantitatively elucidate the mechanical response patterns and underlying mechanisms associated with varying insole Young's modulus. The findings aim to provide robust biomechanical evidence to guide the scientific design and clinical application of personalized functional insoles.

Materials and methods

Geometry design

To evaluate the biomechanical effects of insoles with different material properties on the human foot, the right foot of a healthy adult volunteer (body weight: 60 kg; height: 1.65 m) was selected as the study subject. The study was conducted in accordance with the principles of the Declaration of Helsinki, and written informed consent was obtained from the participant prior to the experiment.A Siemens dual-source CT scanner was used to acquire imaging data of the lower limb (scanning parameters: 120 kV, 240 mA, slice thickness 0.600 mm), generating a total of 780 two-dimensional tomographic images. Based on the CT data, a three-dimensional geometric model of the foot and ankle was reconstructed using MIMICS V10.0 (Materialise Inc., Leuven, Belgium) and exported in STL format. The STL model was subsequently processed in 3-matic Medical 13.0 for mesh smoothing, denoising, subdivision, and defect repair.The cartilage and ligament geometries were constructed in the finite element preprocessing software HyperMesh 2019 (v13.0, Altair Engineering Corp., Michigan, USA). Cartilage was modeled by extruding the bone surface with a thickness equal to half of the minimum inter-bone distance, ranging from 0.5 to 2 mm. All ligaments were defined as tension-only structures and were manually constructed according to anatomical information from a digital anatomy platform and human anatomical atlases. All tissues were assumed to be homogeneous, isotropic, and linearly elastic.To minimize the impact of mesh size on computational accuracy and efficiency, a mesh independence analysis was performed[11]. The element size was gradually reduced from 5 mm to 1 mm, and when the stress deviation between 1 mm and 2 mm elements was below 5%, 2 mm was adopted as the final mesh size. After convergence verification, the final finite element model comprised approximately 549,087 nodes and 3,002,596 elements, as illustrated in Fig. 1.

The assignment of material properties

Finite element simulation of biological tissues is inherently complex because each tissue exhibits unique structural and mechanical characteristics. Their fibrous architecture shows specific spatial orientations and pronounced anisotropic mechanical responses. Many soft tissues exhibit highly nonlinear behaviors, including large deformation (hyperelasticity) and time-dependent responses (viscoelasticity). Therefore, assumptions and simplifications are often required to manage these complexities in computational modeling. In this study, all bones, cartilage, ligaments, and the supporting base plate were modeled as continuous, homogeneous, isotropic, and linearly elastic materials. The base plate was represented as a rigid horizontal plate with a high Young's modulus to simulate the ground support condition[12]. The detailed material properties of each tissue are listed in Table 1.

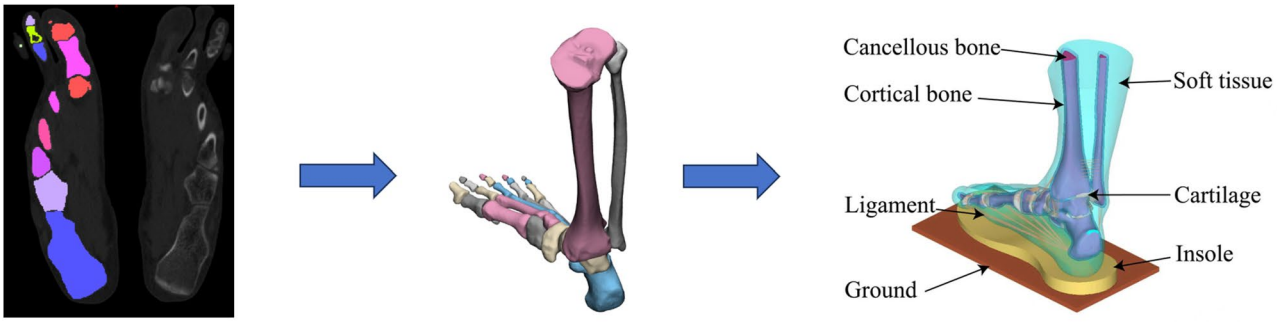

Fig. 1. Three-dimensional reconstruction and finite element model of the human foot with insole.

Components	Young's modulus (MPa)	Poisson's ratio	Element type
Cartilage	1.0	0.42	4-node linear Tetrahedrone
Soft tissue	1.15	0.49	4-node tetrahedrone
Ligament	260	0	2-node linear 3-D Trusse
Cortical bone	7300	0.3	4-node linear Tetrahedrone
Cancellous bone	100	0.3	4-node linear Tetrahedrone
Ground	17,000	0.1	8-node linear bricke

Table 1. Material properties of model components.

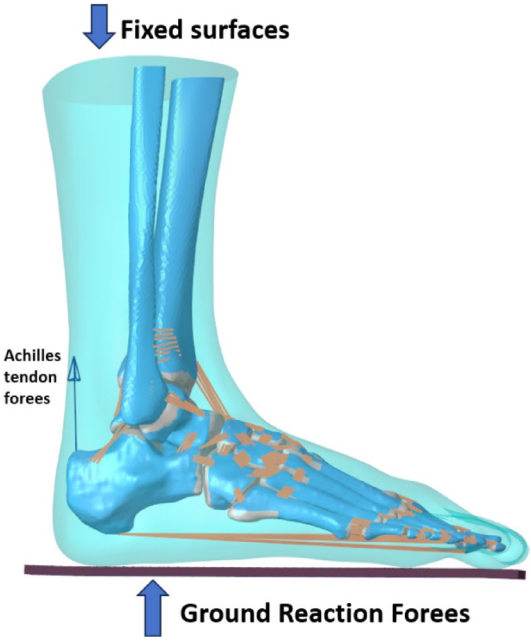

Fig. 2. Finite element boundary conditions of the foot–insole model, including fixed surfaces, Achilles tendon force, and ground reaction force.

Contact pair definition

In the finite element model, proper contact definitions were applied among bones, cartilage, ligament beams, soft tissue, insoles, and the ground to ensure accurate force transmission. The definition of contact pairs and the associated contact area significantly affect the accuracy and convergence of the simulation results. Specifically, the interface between bones and cartilage was defined as node-to-node contact at the proximal side to ensure continuity, and as "No-separation" at the distal side to allow minor sliding without detachment. Both ends of the ligament beams were assigned "Bonded" contact with the bony attachment sites to simulate firm ligament insertion. The plantar surface and insole were also defined as "Bonded" to prevent unrealistic sliding under loading. Finally, the interface between the insole and the rigid ground was defined using a Coulomb friction model with a friction coefficient of 0.6, to closely approximate the physiological load distribution during stance and gait[13].

Definition of boundary conditions and loading

In this study, the subject had a body weight of 60 kg. During static standing, the right foot was assumed to bear approximately half of the body weight (300 N). A vertical force of 300 N was applied upward through the rigid ground to simulate the plantar ground reaction force under balanced stance. The distal ends of the tibia and fibula were fully constrained to represent physiological ankle support.Additionally, an upward tensile force of 150 N was applied along the Achilles tendon to simulate the physiological tendon reaction. This value was derived from Simkin et al.[14], who reported that the Achilles tendon force is approximately 50% of the load borne by the foot during quiet standing. Accordingly, the combined skeletal and tendon loading was represented by a net vertical force of 300 N applied at the plantar pressure center and a 150 N Achilles tendon reaction force, closely reproducing the physiological loading scenario. All loads were applied via point loads and uniform pressure distributions. The specific boundary and loading conditions are illustrated in Fig. 2.

Validation

To validate the reliability of the finite element (FE) model, plantar pressure measurements were obtained from the volunteer who underwent the initial CT scanning. The simulated plantar stress distribution from the FE model closely matched the experimental measurements. Specifically, the peak plantar pressure was 0.2217 MPa in the in vivo measurement and 0.234 MPa in the FE simulation (Fig. 3), yielding an error of approximately 2%. Both the experimental and simulated results showed the peak stress region located at the central heel, and the overall distribution trends were consistent. In line with previous studies on plantar FE model development and validation[15], although variations exist in mesh density, boundary constraints, and loading configurations, the present model demonstrated sufficient biomechanical fidelity. This confirms the model's validity and provides a robust basis for subsequent simulations of insole material effects.

Finite element simulation of insole models

To investigate the biomechanical effects of insoles with varying material properties on plantar stress, we simulated different insole stiffness levels by adjusting their Young's modulus. Six insole models were constructed with elastic moduli of 100, 260, 1,000, 3,000, 5,000, and 500,000 MPa, The Poisson's ratio for all insole materials was assumed to be 0.45. The value of 500,000 MPa was chosen as a theoretical rigid boundary condition, intended to explore the impact of very high material stiffness on the simulation outcomes. It was used to assess whether increasing Young's modulus beyond a certain point would continue to affect the final calculation results. Using four-node tetrahedral elements. Previous studies have indicated that insoles exert the greatest influence on plantar loading during the static stance phase and the forefoot contact phase of gait[16]. After validating the foot finite element model, the insole models were incorporated into the system, and simulations were conducted under the same boundary conditions. Plantar stress distributions and stresses in key foot structures were analyzed to systematically assess the influence of insole stiffness on foot biomechanics (Fig. 4).

Results

Biomechanical response under static bilateral stance

Under static bilateral stance, the effect of insole Young's modulus on foot biomechanics was modest but followed a consistent trend (Fig. 5; Table 2). As the modulus increased from 100 MPa to 500,000 MPa, foot displacement decreased from 3.154 mm to 3.034 mm (3.8% reduction); the peak von Mises stress at the medial process of the calcaneal tuberosity decreased from 82.24 MPa to 79.50 MPa (3.3% reduction); metatarsal peak stress decreased from 19.76 MPa to 19.63 MPa (0.7% reduction); and peak plantar stress decreased from 0.426 MPa to 0.405 MPa (4.9% reduction). Overall, the improvement under static loading was less than 5%, suggesting limited sensitivity of foot loading to insole stiffness during quiet standing.

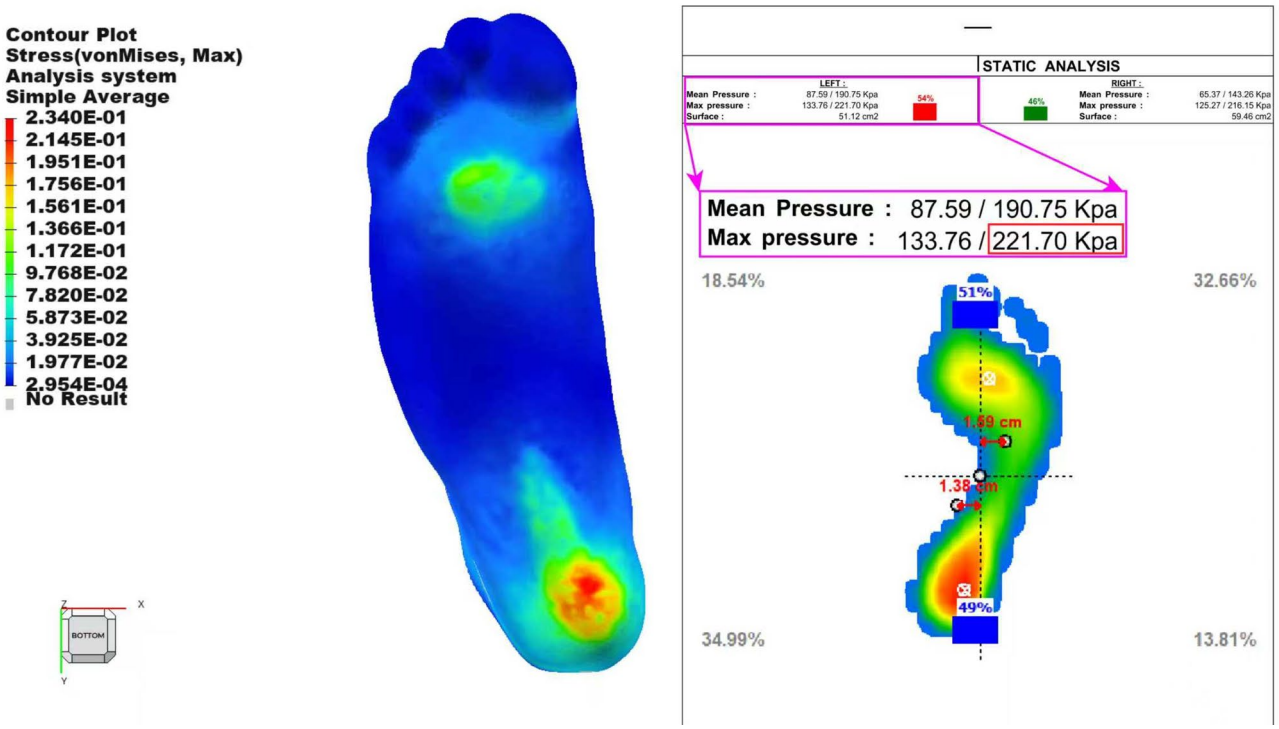

Fig. 3. Validation of the finite element model by comparison with experimental plantar pressure measurements.

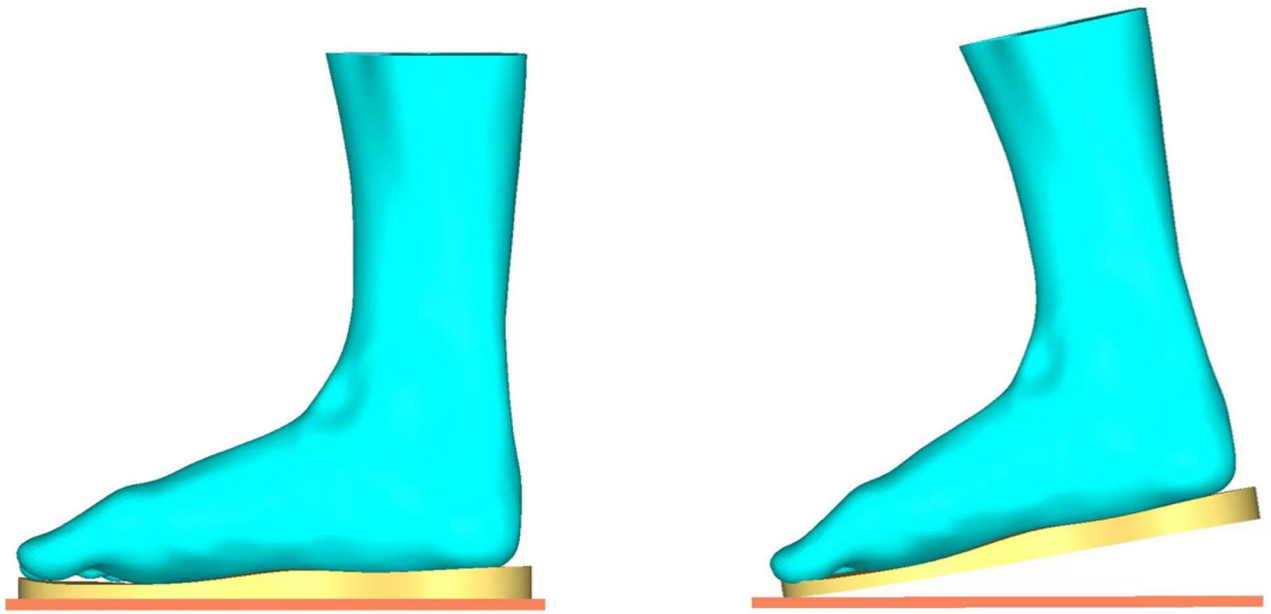

Fig. 4. Simulation of two typical loading conditions: static bilateral stance (left) and gait forefoot contact (right).

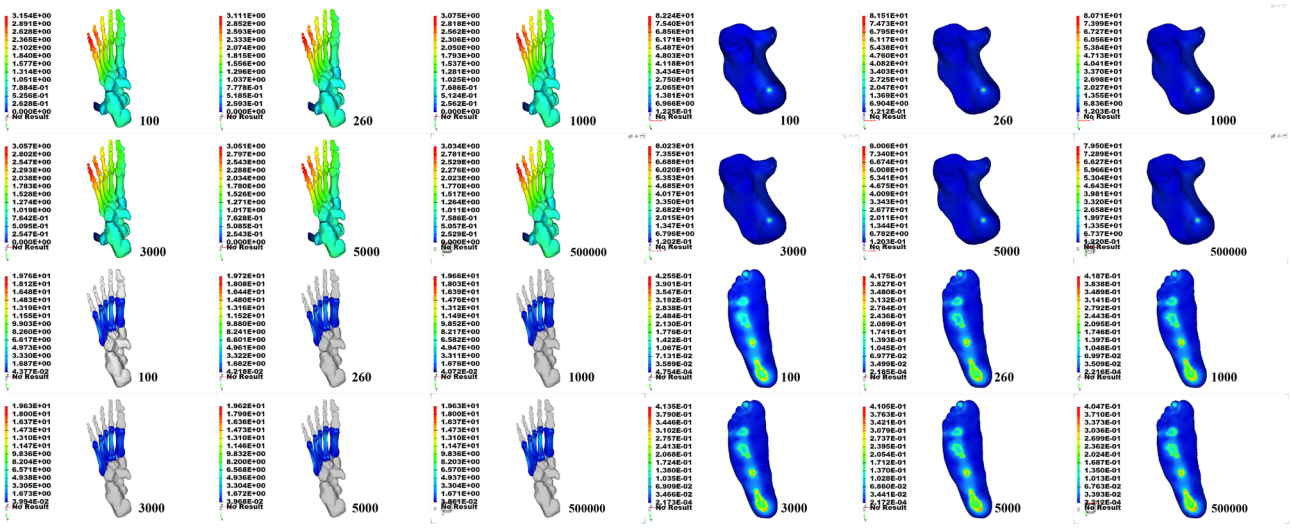

Fig. 5. Finite element analysis of foot biomechanics with insoles of varying Young's moduli under static bilateral stance.

Insole material(MPa)	Foot displacement (mm)	Medial process of the calcaneal tuberosity stress (MPa)	Metatarsal stress (MPa)	Plantar stress (MPa)
100	3.154	82.240	19.760	0.426
260	3.111	81.510	19.720	0.418
1000	3.075	80.710	19.660	0.419
3000	3.057	80.230	19.630	0.414
5000	3.051	80.060	19.620	0.411
500,000	3.034	79.500	19.630	0.405

Table 2. Foot displacement and tissue stresses under static bilateral stance for insoles with varying young's moduli.

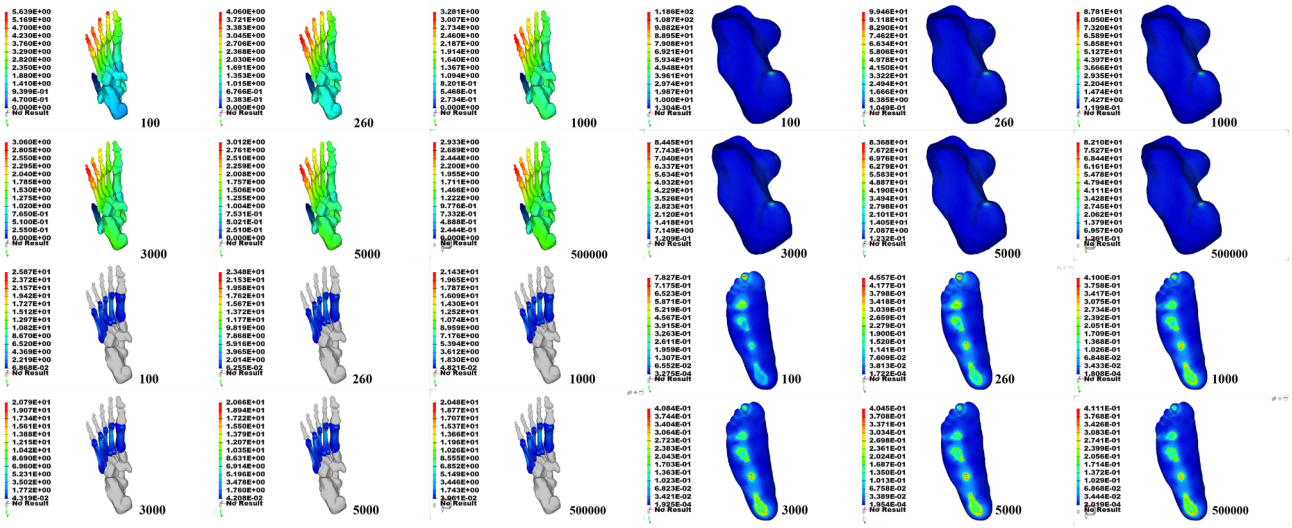

Fig. 6. Finite element analysis of foot biomechanics with insoles of varying Young's moduli during the forefoot loading phase of gait.

Insole material(MPa)	Foot displacement (mm)	Medial process of the calcaneal tuberosity stress (MPa)	Metatarsal stress (MPa)	Plantar stress (MPa)
100	5.639	118.600	25.870	0.783
260	4.060	99.460	23.480	0.456
1000	3.281	87.810	21.430	0.410
3000	3.060	84.450	20.790	0.408
5000	3.012	83.680	20.660	0.405
500,000	2.933	82.100	20.480	0.411

Table 3. Foot displacement and tissue stresses under forefoot contact phase of gait for insoles with varying young's moduli.

Biomechanical response during forefoot contact in gait

During the forefoot contact phase of gait, the foot exhibited markedly greater sensitivity to insole stiffness (Fig. 6; Table 3). As the modulus increased from 100 MPa to 500,000 MPa, foot displacement decreased substantially from 5.639 mm to 2.933 mm (48.0% reduction); peak von Mises stress at the medial calcaneal process decreased from 118.6 MPa to 82.1 MPa (30.8% reduction); metatarsal peak stress decreased from 25.87 MPa to 20.48 MPa (20.8% reduction); and peak plantar stress decreased markedly from 0.783 MPa to 0.411 MPa (47.5% reduction). Compared with static stance, stress reduction was much more pronounced under dynamic loading, indicating that stiffer insoles provide enhanced arch support and more effective plantar load redistribution during gait.

Overall trends and biomechanical implications

Across both loading conditions, finite element analysis demonstrated that higher insole Young's modulus reduces foot displacement and peak stresses in key tissues, enhancing arch stability and redistributing plantar loads. However, when the modulus exceeded approximately 3,000 MPa, the rate of stress and displacement reduction diminished, presenting a "plateau effect." This finding suggests that excessively rigid insoles offer no additional biomechanical benefit (Fig. 7).

Discussion

This study employed three-dimensional finite element analysis to systematically quantify the biomechanical effects of insoles with varying Young's moduli (100 MPa to 500,000 MPa) on key foot tissues. The results demonstrated that as insole stiffness increased, both overall foot displacement and local tissue stresses significantly decreased, with the most pronounced effects observed during the forefoot contact phase of gait. This study clearly revealed the quantitative influence of insole stiffness on foot biomechanics during gait, including reductions in foot displacement (48.0%), peak stress at the medial process of the calcaneal tuberosity (30.8%), metatarsal peak stress (20.8%), and peak plantar pressure (47.5%). Unless otherwise stated, all percentage changes are relative within-model comparisons across stiffness levels and should be interpreted as upper-bound theoretical predictions, not as direct clinical values. Compared with previous finite element studies that primarily focused on static or simplified gait conditions[7,17,18], this work systematically evaluated both stress and displacement responses under

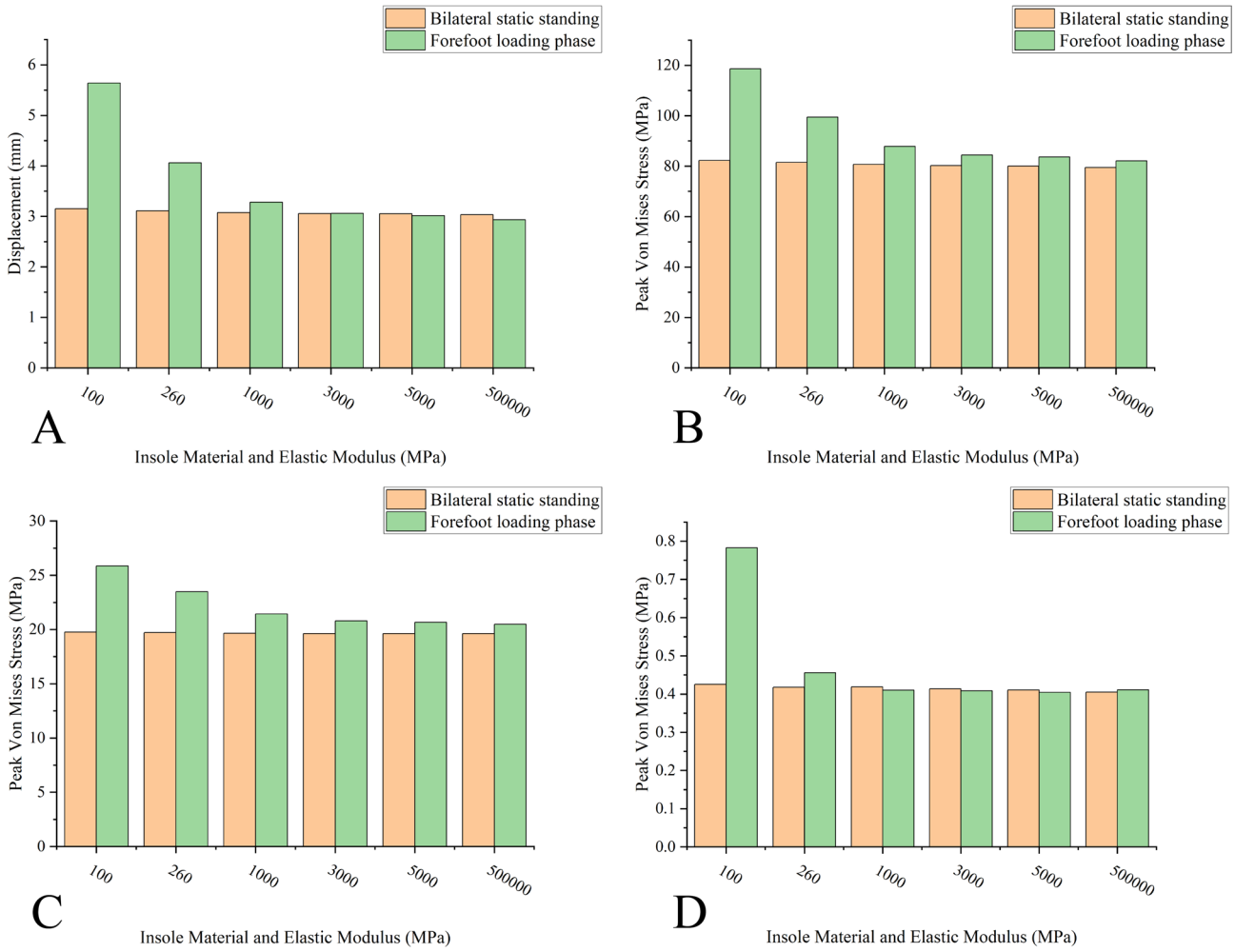

Fig. 7. Biomechanical responses of the foot under different insole materials with varying Young's moduli during static and dynamic loading conditions. (**A**) Foot displacement; (**B**) Peak von Mises stress at the medial process of the calcaneal tuberosity; (**C**) Peak metatarsal stress; (**D**) Peak plantar stress. Results are compared between bilateral static standing and forefoot loading phase of gait.

typical static and dynamic loading, providing direct and robust biomechanical evidence for the functional insole design in dynamic scenarios.

This outcome can be attributed to the pronounced influence of insole Young's modulus on arch support and the biomechanical response patterns of plantar soft tissues. Insoles with low Young's modulus undergo substantial elastic deformation under load, resulting in excessive arch collapse and overstretching of plantar soft tissues, thereby increasing the risk of localized stress concentration in the plantar fascia and metatarsals. This phenomenon aligns with the findings of McDonald et al.[19], who reported that the plantar fascia experiences a characteristic elastic stretch–shortening cycle during the support phase, with the majority of strain arising from arch compression, underscoring the pivotal role of the arch as an elastic "spring" structure in weight-bearing activities. Excessively soft insoles provide insufficient arch support, which not only diminishes the energy storage and return functions of this spring-like mechanism but may also impose additional tensile loads on the plantar fascia, heightening the risk of fatigue accumulation and tissue injury. Through the quantitative comparison of insoles with different Young's moduli, this study further elucidates the dynamic coupling between plantar soft tissues and external rigid support, and confirms that moderately increasing insole stiffness under gait loading can substantially reduce stresses on key foot structures. This finding is consistent with the work of Luo et al.[20], who demonstrated—via finite element analysis and indentation experiments—that optimizing insole elasticity and structural design can markedly redistribute internal and surface plantar stresses, strains, and strain energy density (SED), thereby mitigating the risk of soft tissue injury. The quantitative evidence from the present study further establishes that increasing insole Young's modulus effectively limits plantar structural deformation and reduces peak local stresses, providing robust biomechanical support for the mechanism of insole-mediated arch support.

Existing studies predominantly emphasize the role of functional insoles in the prevention and rehabilitation of plantar fasciitis, metatarsalgia, and diabetic foot[21,22]. However, recommendations regarding the appropriate range of insole Young's modulus largely rely on empirical experience, lacking clear quantitative support. The

present study identifies a "threshold effect" for insole stiffness: when the Young's modulus exceeds approximately 3,000 MPa, the reductions in foot displacement and key tissue stresses become markedly attenuated, exhibiting a typical "plateau effect" or "diminishing marginal returns." This finding suggests that insole design should not pursue unlimited stiffness but instead achieve an optimal balance between biomechanical load reduction and wearing comfort[23,24]. Although similar phenomena have been qualitatively reported, most rely on subjective comfort assessment rather than quantitative evidence[25–27]. Casado et al.[28] observed that harder insoles reduced plantar pressures and improved comfort in motorcycling scenarios, which aligns with our results, yet no optimal stiffness range was provided. By contrast, this study quantitatively defines the threshold range of insole Young's modulus via finite element analysis, providing objective biomechanical evidence for personalized insole design. Clinically, we recommend selecting the optimal stiffness range according to patient type: (i) medium-to-high modulus insoles (1,000–3,000 MPa) are suitable for plantar fasciitis or high-stress sports injuries to reduce plantar fascia and metatarsal stress and mitigate recurrence risk; (ii) flexible insoles (< 1000 MPa) are preferable for daily comfort and low-load activities to enhance cushioning and wear experience; and (iii) for personalized applications, "modulus matching" can be achieved by integrating foot imaging with finite element simulation to avoid excessive stiffness compromising comfort. Although our results indicate that as insole stiffness increases, both foot displacement and stress decrease, this finding may seem to contradict the common use of softer insole materials in clinical practice. In the finite element analysis, stiffer insole materials provided more support, reducing the deformation of foot soft tissues and thereby lowering plantar loading and stress. However, in practice, softer insole materials are widely used for their better comfort and shock absorption properties. This discrepancy primarily stems from the idealized assumptions in our study. We chose linear elastic models and simplified static loading conditions to explore the basic effects of insole stiffness on foot biomechanics. In reality, insole design considers not only stiffness but also balances comfort, adaptability, and individual needs. While our simulations show biomechanical advantages of stiffer insoles, comfort and shock absorption are often prioritized by many users in actual designs. Future functional insole design should fully consider this "threshold effect," ensuring effective biomechanical load mitigation while maintaining wearability, thereby facilitating the transition from empirical to precise and individualized insole development.

Despite providing clear biomechanical evidence, this study has several limitations. First, the finite element model was based on CT data from a single healthy male, without accounting for variations in sex, age, body weight, or foot conditions (such as flatfoot or high-arched feet), which could influence foot biomechanics and limit the generalizability of the findings. Second, the study only simulated two loading conditions—static bilateral stance and forefoot contact during gait—without considering more complex dynamic scenarios, such as running or jumping, which restricts the comprehensive representation of dynamic foot loading. Third, the model used linear elasticity to simulate soft tissues, a simplification that fails to capture the nonlinear behavior of soft tissues, especially under large deformations and dynamic loading conditions. Additionally, muscle forces were not included in the model, though muscle forces are crucial biomechanical factors in gait. Future studies should include more diverse foot types, expand sample sizes, and simulate a broader range of dynamic scenarios to enhance the generalizability of the results. Incorporating musculoskeletal modeling and nonlinear material properties (such as viscoelasticity or hyperelasticity) will further improve the accuracy and clinical relevance of the simulations. While these simplifications exist, the current model results still provide valuable preliminary insights and offer effective reference value for insole design.

Conclusion

This study systematically quantified the biomechanical effects of insole Young's modulus on key foot tissues using three-dimensional finite element analysis. The results demonstrate that increasing insole stiffness significantly reduces foot displacement and tissue stresses, with the most pronounced effect occurring during forefoot contact in gait. Moreover, a threshold effect was identified at approximately 3,000 MPa, providing robust biomechanical evidence to guide the scientific material selection and personalized design of functional insoles.

Data availability

All data generated or analysed during this study are included in this published article and its supplementary information files.

Received: 9 August 2025; Accepted: 13 November 2025
Published online: 29 December 2025

References

1. Zhang, L. et al. The relationship between calcaneal spur type and plantar fasciitis in Chinese population. *Biomed. Res. Int.* **2020**, 5679629 (2020).
2. Heide, M., Mork, M., Roe, C., Brox, J. I. & Fenne Hoksrud, A. The effectiveness of radial extracorporeal shock wave therapy (rESWT), sham-rESWT, standardised exercise programme or usual care for patients with plantar fasciopathy: study protocol for a double-blind, randomised, sham-controlled trial. *Trials* **21**(1), 589 (2020).
3. Wilke, J., Vleeming, A. & Wearing, S. Overuse injury: the result of pathologically altered myofascial force transmission? *Exerc. Sport Sci. Rev.* **47**(4), 230–236 (2019).
4. Ahadi, T. et al. The effect of dextrose prolotherapy versus placebo/other non-surgical treatments on pain in chronic plantar fasciitis: a systematic review and meta-analysis of clinical trials. *J. Foot Ankle Res.* **16**(1), 5 (2023).
5. Jin, H., Xu, R., Wang, S. & Wang, J. Use of 3D-printed heel support insoles based on arch lift improves foot pressure distribution in healthy people. *Med. Sci. Monit.* **25**, 7175–7181 (2019).
6. Collings, R., Freeman, J., Latour, J. M. & Paton, J. Footwear and insole design features for offloading the diabetic at risk foot-A systematic review and meta-analyses. *Endocrinol. Diabetes Metab.* **4**(1), e00132 (2021).

7. Yang, Z. et al. Design feature combinations effects of running shoe on plantar pressure during heel landing: A finite element analysis with Taguchi optimization approach. *Front. Bioeng. Biotechnol.* **10**, 959842 (2022).
8. Wang, S. et al. Finite element analysis of the initial stability of arthroscopic ankle arthrodesis with three-screw fixation: posteromedial versus posterolateral home-run screw. *J. Orthop. Surg. Res.* **15**(1), 252 (2020).
9. Zhang, Q., Zhang, Y., Huang, J., Teo, E. C. & Gu, Y. Effect of displacement degree of distal chevron osteotomy on metatarsal stress: A finite element method. *Biology*. **11**(1) (2022).
10. Yu, J. et al. Finite element stress analysis of the bearing component and bone resected surfaces for total ankle replacement with different implant material combinations. *BMC Musculoskelet. Disord.* **23**(1), 70 (2022).
11. Robinson, D. L. et al. The application of finite element modelling based on clinical pQCT for classification of fracture status. *Biomech. Model. Mechanobiol.* **18**(1), 245–260 (2019).
12. Liu, W. et al. Biomechanical application of finite elements in the orthopedics of stiff clubfoot. *BMC Musculoskelet. Disord.* **23**(1), 1112 (2022).
13. Ito, K. et al. Comparative functional morphology of human and chimpanzee feet based on three-dimensional finite element analysis. *Front. Bioeng. Biotechnol.* **9**, 760486 (2021).
14. Simkin, A., Arcan, M. & Brull, M. A structural model of the human foot. In *Biomechanics: Current Interdisciplinary Research: Selected proceedings of the Fourth Meeting of the European Society of Biomechanics in Collaboration with the European Society of Biomaterials, September 24–26, 1984* (eds Perren, S. M. et al.) 339–344. (Springer Netherlands, 1985).
15. Song, Y. et al. Development and validation of a subject-specific coupled model for foot and sports shoe complex: A pilot computational study. *Bioengineering*. **9**(10) (2022).
16. Rattanasak, A. et al. Real-Time gait phase detection using wearable sensors for transtibial prosthesis based on a kNN algorithm. *Sensors*. **22**(11) (2022).
17. Gerrard, J. M., Bonanno, D. R., Whittaker, G. A. & Landorf, K. B. Effect of different orthotic materials on plantar pressures: a systematic review. *J. Foot Ankle Res.* **13**(1), 35 (2020).
18. Hudak, Y. F. et al. A novel workflow to fabricate a patient-specific 3D printed accommodative foot orthosis with personalized latticed metamaterial. *Med. Eng. Phys.* **104**, 103802 (2022).
19. McDonald, K. A. et al. The role of arch compression and metatarsophalangeal joint dynamics in modulating plantar fascia strain in running. *PLoS One*. **11**(4), e0152602 (2016).
20. Luo, G., Houston, V. L., Garbarini, M. A., Beattie, A. C. & Thongpop, C. Finite element analysis of heel pad with insoles. *J. Biomech.* **44**(8), 1559–1565 (2011).
21. Hähni, M., Hirschmüller, A. & Baur, H. The effect of foot orthoses with forefoot cushioning or metatarsal pad on forefoot peak plantar pressure in running. *J. Foot Ankle Res.* **9**, 44 (2016).
22. Collings, R., Freeman, J., Latour, J. M., Hosking, J. & Paton, J. Insoles to ease plantar pressure in people with diabetes and peripheral neuropathy: a feasibility randomised controlled trial with an embedded qualitative study. *Pilot Feasibility Stud.* **9**(1), 20 (2023).
23. Wang, Y., Lam, W. K., Cheung, C. H. & Leung, A. K. Effect of red arch-support insoles on subjective comfort and movement biomechanics in various landing heights. *Int J. Environ. Res. Public. Health* **17**(7) (2020).
24. Harte, R. et al. A Multi-Stage human factors and comfort assessment of instrumented insoles designed for use in a connected health infrastructure. *J. Pers. Med.* **5**(4), 487–508 (2015).
25. Melia, G., Siegkas, P., Levick, J. & Apps, C. Insoles of uniform softer material reduced plantar pressure compared to dual-material insoles during regular and loaded gait. *Appl. Ergon.* **91**, 103298 (2021).
26. Paton, J., Glasser, S., Collings, R. & Marsden, J. Getting the right balance: insole design alters the static balance of people with diabetes and neuropathy. *J. Foot Ankle Res.* **9**, 40 (2016).
27. Yi, T. I., Lee, E. C., Son, N. H. & Sohn, M. K. Comparison of the forefoot pressure-relieving effects of foot orthoses. *Yonsei Med. J.* **63**(9), 864–872 (2022).
28. Casado-Hernández, I., Becerro-de-Bengoa-Vallejo, R., López-López, D., Gómez-Bernal, A. & Losa-Iglesias, M. E. Aluminum foot insoles reduce plantar forefoot pressure and increase foot comfort for motorcyclists. *Prosthet. Orthot. Int.* **42**(6), 606–611 (2018).

Acknowledgements

The author would like to thank Prof. Wencui Li for his guidance and input during the project.

Author contributions

LWC had full access to all the data in the study and took responsibility for the integrity of the data and the accuracy of data analysis. LRB, and LW contributed to conducting the experiment and writing the manuscript. TX, WGH and LJQ contributed to the study design, ZZ collected experimental data. All authors read and approved the final version of the manuscript.

Funding

Supported by Sanming Project of Medicine in Shenzhen (No.SZSM202311008).

Declarations

Ethics approval and consent to participate

All experimental protocols were approved by the Ethics Committee of Shenzhen Second People's Hospital (Ethical approval number: 2024-398-01PJ). The study was conducted according to the principles of the Declaration of Helsinki, and participants gave written informed consent to participate in our research.

Competing interests

The authors declare no competing interests.

Additional information

Supplementary Information The online version contains supplementary material available at https://doi.org/10.1038/s41598-025-28905-7.

Correspondence and requests for materials should be addressed to W.L. or W.L.